

Excitation Energy Dependence of Fluorescence Intermittency in CdSe/ZnS Core–Shell Nanocrystals

Catherine H. Crouch,^{*,†} Robert Mohr,[†] Thomas Emmons,[†] Siying Wang,[‡] and Marija Drndić[‡]

Department of Physics and Astronomy, Swarthmore College, Swarthmore, Pennsylvania 19081, and
Department of Physics and Astronomy, University of Pennsylvania, Philadelphia, Pennsylvania 19104

Received: November 27, 2008; Revised Manuscript Received: April 25, 2009

We report measurements of the excitation energy dependence of the fluorescence intermittency of single CdSe/ZnS core/shell nanocrystals (NCs), using two different sizes of NCs and three different excitation energies. The lowest excitation energy corresponds to exciting the smaller size NC at its optical band gap, so we examine both excitation at the band gap and at varying energies above the band gap. We find that off-time probability distributions follow a power law with exponent roughly -1.5 regardless of NC size or excitation energy. The on-time probability distributions follow a truncated power law with a power-law exponent that again does not depend on size or energy. With comparable absorption rate, the truncation times for the larger nanocrystals are very similar when excited either 270 or 480 meV above the band gap but shorten for near-ultraviolet excitation 1 eV above the band gap. For the smaller nanocrystals, the truncation times are comparable whether excited at the band gap or 270 meV above. Our findings support a spectral diffusion-controlled model for blinking and are consistent with the existence of a quasicontinuous manifold of excited states with altered emission dynamics above the $1P_e$ state; they also indicate a change in emission dynamics at very high excess energy.

Introduction

Fluorescence intermittency, or blinking, irregular switching between bright and dark states under continuous illumination, appears to be a nearly universal property of single fluorophores.^{1,2} Intermittency has been observed in fluorophores ranging from single organic molecules and green fluorescent protein to quantum dots, rods, and wires. In most of these systems, the durations of time spent emitting (“on”) or dark (“off”) display power law probability density distributions over many orders of magnitude in time, rather than the exponential distributions that would be expected of a two-level, single-rate process.^{1,2} Although much experimental and theoretical progress has been made, there are still many unanswered questions about the underlying mechanism. In addition, intermittency poses a practical obstacle to many potential applications of single-emitter fluorescence, such as fluorescence resonance energy transfer measurements, particle tracking, and single-photon sources.¹ Understanding fluorescence intermittency is thus a matter of both fundamental interest and practical value.

Colloidally synthesized semiconductor nanocrystals (NCs) provide a convenient system in which to study many properties of single fluorophores, because of their high quantum yield, broad absorption band, and stability against photobleaching. In particular, fluorescence from single CdSe/ZnS core–shell NCs has been measured for 1 h or more. Such measurements have established that the durations of off-events, or off times, t_{off} , follow a power law distribution with probability density $P(t_{\text{off}}) = At_{\text{off}}^{m_{\text{off}}}$, over six decades in time.³ The on-time durations follow a power law distribution for durations up to several seconds but then fall below the power law for longer times.⁴

Quantitatively, several studies have found the on times, t_{on} , to follow a truncated power law, $P(t_{\text{on}}) = At_{\text{on}}^{-m_{\text{on}}}e^{-t_{\text{on}}/\tau_{\text{on}}}$, with the “truncation time” (also called the “saturation time”) τ_{on} characterizing the time scale on which exponential distributions are observed;^{5,6} this form is predicted by spectral diffusion models for blinking.^{7–9} This parameter τ_{on} has been found to depend on excitation intensity,^{4,10,11} as well as aspect ratio, in a study of rod-shaped nanocrystals,⁵ and temperature.⁴ The intensity dependence of τ_{on} is one of several indications that blinking is a light-driven process.^{2,11}

A variety of theoretical models have been proposed to explain nanocrystal blinking. A common feature of most models, based on the original theory of Efros and Rosen,¹² is that the transition from a bright (“on”) state to a dark (“off”) state occurs when a photoexcited electron or hole escapes from the NC to a state in the environment or at the surface of the NC, leaving the core of the NC charged. In the charged core, the nonradiative recombination rate is strongly enhanced compared to the radiative rate via Auger-like processes, so a charged NC is dark. The “on” state is restored when an electron or hole returns and restores electrical neutrality to the core. Models differ in how they account for the broad distributions of electron escape and recapture rates that are required for power-law statistics. One class of models accounts for this distribution through spectral diffusion of the NC and trap states,^{4,7} while other models involve fluctuations in tunneling barriers between the core and the traps,³ fluctuations in the nonradiative rate,^{9,13,14} and dynamic self-trapping.^{1,15}

One aspect of blinking that has been studied relatively little, with just a few recent studies,^{6,11} is the role of the energy of excitation in nanocrystal blinking. The band structure of semiconductor NCs gives rise to a quasicontinuous absorption spectrum well above the band gap; most studies of single-NC fluorescence intermittency have been performed using a con-

* To whom correspondence should be addressed. E-mail: ccrouch1@swarthmore.edu, phone: (610) 328-8386, fax: (610) 328-7895.

[†] Swarthmore College.

[‡] University of Pennsylvania.

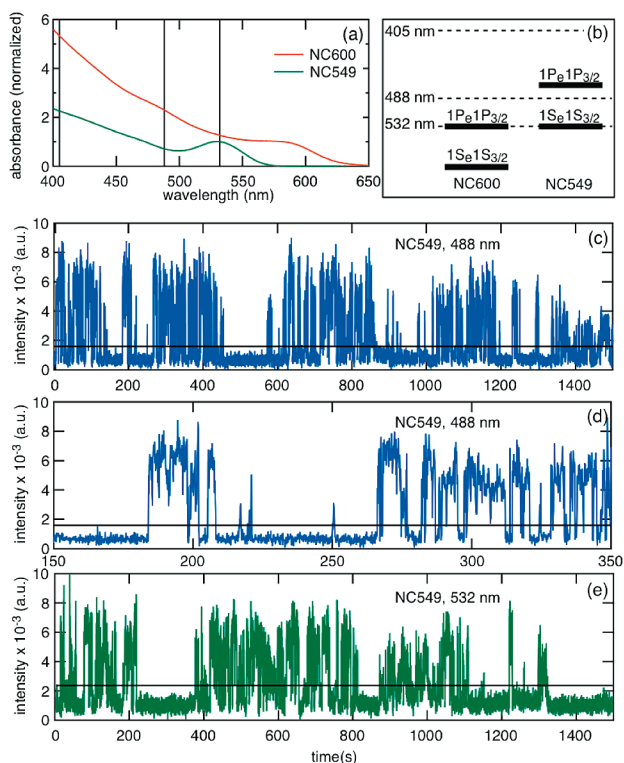


Figure 1. (a) Absorbance vs wavelength for NC549 and NC600 bulk samples. Absorbance is normalized to unity at the first absorption peak for both samples. Vertical lines indicate 532, 488, and 405 nm laser excitation wavelengths. (b) Schematic energy diagram (to scale) showing three excitation energies, bulk absorption edge (1S_e1S_{3/2}), and 1P_e1P_{3/2} states for the two sizes of NC studied, based on Norris and Bawendi;²² other energy levels for NCs are not shown. (c) Representative intensity vs time data, $I(t)$, obtained from a single NC549 using 488 nm excitation, with the threshold above which the NC is considered to be “on” indicated by the solid horizontal line. (d) Expanded region of data shown in (c). (e) Representative intensity vs time data, $I(t)$, obtained from a single NC549 using 532 nm excitation, with the threshold above which the NC is considered to be “on” indicated by the solid horizontal line. Threshold and intensity level is somewhat different than in (c) due to camera settings.

venient excitation wavelength well above the absorption edge. However, information about how blinking depends on the position of the excitation within the NC energy level structure should shed light on the mechanism. In particular, measurements of blinking dependence at excitation energies close to and well above the band gap will indicate whether the state into which the electron is excited affects the blinking dynamics.

Here we report measurements of fluorescence blinking of two different sizes of core/shell NCs at several different wavelengths. For the larger size, with bulk absorption peak near 585 nm and emission peak near 600 nm,¹⁶ we excited the NCs at three different wavelengths (532 nm, 488 nm, and 405 nm), all at least 250 meV above the first absorption peak for the bulk solution; for the smaller size, with bulk absorption peak at 531 nm and bulk emission peak at 549 nm, we excited the NCs at 532 and 488 nm. (The excitation conditions are displayed in Figure 1a,b and energies provided in Table 1. The smaller NCs bleached too rapidly with the 405 nm excitation for us to obtain useful data.) For both sizes of NCs, we observe the same off-time power law exponent for all excitation energies. We do, however, find that excitation at the band gap increases the fraction of time the NC is dark. For each size, we observe similar on-time probability distributions with 532 and 488 nm excitation; however, at comparable photon absorption rates, the larger

TABLE 1: Energies of Excitations, Bulk Absorption Edges, and 1P_eP_{3/2} States^a

sample	bulk absorption edge (eV)	1P _e P _{3/2} state, ^a (eV)
NC549	2.33	2.61
NC600	2.06	2.33

laser wavelength (nm)	laser energy (eV)
532	2.33
488	2.54
405	3.06

^a Based on Norris and Bawendi.²²

NCs show a power law exponent to the on-time distribution lower than that of the smaller NCs, reflecting more total time spent on. For the larger NCs, exciting at 405 nm gives a shorter cutoff to the on-time distribution than exciting at 532 or 488 nm.

Experimental Methods

We performed wide-field fluorescence imaging of many single NCs simultaneously, using an epifluorescence microscope (Olympus) with a 100×, 0.95 NA dry objective or a 60×, 1.42 NA oil immersion objective. Core-shell CdSe/ZnS nanocrystals were purchased from Evident Technologies. Samples were prepared for imaging by spin-casting a very dilute toluene solution of NCs onto mica or glass substrates. The concentration of the solution was chosen so that individual NCs were typically separated by a few micrometers. Mica substrates used with the dry objective were freshly cleaved; glass coverslips used with the oil objective were cleaned in a mixture of sulfuric acid and hydrogen peroxide.

The sample was illuminated by continuous wave (cw) laser light from one of three different laser sources: a 532 nm solid-state laser (Coherent Compass), a 488 nm solid-state laser (Coherent Sapphire), or a 405 nm diode laser (Coherent CUBE). The diode laser was passed through an air-launch fiber system to produce a TEM₀₀ beam profile. Each laser was expanded and focused near the back aperture of the microscope objective to illuminate an extended area of the microscope field of view. Samples were measured at room temperature in air immediately after preparation to minimize sample degradation. Fluorescence movies were captured by a thermoelectrically cooled EM-CCD camera (Princeton Instruments Cascade 512F or Photonmax) at 10 frames per second. All measurements presented in this paper lasted 1500 s unless otherwise specified. The fluorescence intensity $I(t)$ of each emitter was calculated from each frame throughout the entire movie.

Results

Intensity Measurements. Figure 1 shows representative examples of the time-dependent fluorescence $I(t)$ from a single one of the smaller NCs (hereafter NC549 to indicate the bulk emission center wavelength) obtained with 488 nm excitation at 240 W/cm² (Figure 1c,d) or 532 nm excitation at 185 W/cm² (Figure 1e). These excitation intensities correspond to photon absorption rates of 0.13 MHz at 488 nm and 0.14 MHz at 532 nm. We set the intensities to correspond to equivalent photon absorption rates at the two wavelengths, as we have observed that on-time probability distributions vary gradually with excitation intensity, while the off-time distributions are unaffected by intensity. The intensities were determined by finding the intensities at which a monolayer film of the larger nanocrystals produced the same fluorescence intensity with both wavelengths and adjusting by the measured absorption for the

smaller nanocrystals. (The larger nanocrystals were used because their quantum yield is relatively insensitive to wavelength over the range of interest.^{17,18}) Subsequent calculation of absorption rate from illumination intensity and nanocrystal absorption cross-sections calculated by the method of Yu et al.¹⁹ confirmed agreement of the absorption rate within 20%.

The threshold used to distinguish “off” and “on” is also indicated in Figure 1c–e (black horizontal line). To set the threshold, we measured the range ΔI_{dark} and standard deviation σ_{dark} of the background signal obtained from dark regions of the sample; the threshold for each NC was then set to be $\Delta I_{\text{dark}} + \sigma_{\text{dark}}$ above the minimum intensity recorded for that NC. The threshold is slightly different for the two data sets because a higher camera gain setting was used with the 532 nm excitation.

Data like those shown in Figure 1 were obtained from 64 single NC549 at 488 nm and from 47 single NC549 at 532 nm, and from each $I(t)$, a histogram of on- and off-event durations was calculated. Probability densities $P(\tau_{\text{on}})$ and $P(\tau_{\text{off}})$ were then calculated from these histograms as described in our previous work,⁵ using the weighting scheme developed by Kuno and co-workers.³

Off-Time Distributions: Power-Law Exponents and Total Off Time. Regardless of excitation energy and intensity, the off probability densities for all individual nanocrystals follow a power law distribution $P(t_{\text{off}}) = At_{\text{off}}^{-m_{\text{off}}}$ with an exponent m_{off} close to 1.5; exponent values were obtained from linear fits to $\log[P(t_{\text{off}})]$ vs $\log(t_{\text{off}})$ (shown in Figure 2). Parts a and b of Figure 2 show the off-probability densities for the data of Figure 1c,e; similar distributions were obtained from each of the other individual NCs measured. The insets to Figure 2a,b show the histograms of m_{off} values obtained from individual NC549 with 488 and 532 nm excitation, respectively. The average values obtained from the individual NCs are $m_{\text{off}} = 1.5$ (standard deviation = 0.1) for both 488 and 532 nm excitation. Thus, there appears to be no significant difference between the power law exponents obtained with 488 and 532 nm.

Likewise, measurements on the larger NCs (NC600) with any of the three wavelengths (532, 488, and 405 nm) give essentially the same results for the off-time probability distributions. Again the excitation energy has no significant effect on the slopes of the off-time distributions. Measuring fluorescence with the 405 nm excitation required a significantly lower excitation rate to avoid bleaching the NCs (0.13 MHz, corresponding to 30 W/cm² at 405 nm and 85 W/cm² at 532 nm; measurements comparing 532 and 488 nm were carried out at absorption rates of 0.73 MHz at 488 nm and 0.60 MHz at 532 nm, corresponding to 190 W/cm² at 488 nm and 250 W/cm² at 532 nm). We therefore measured with both 532 and 405 nm at this lower excitation rate. In order to obtain good signal-to-noise with the reduced signal level, a glass substrate was used with a 1.4 NA oil immersion objective with higher collection efficiency. The off-time distributions obtained with all three energies, regardless of excitation rate, were comparable. The results of the fits for both sizes of nanocrystals and all wavelengths are provided in Table 2.

We also examined the total time for which each individual NC is dark. Figure 3 shows histograms of the total off time observed from each individual NC, with average values and standard deviations included in the figure legends. For the smaller NCs (NC549), for which 532 nm excitation falls at the lowest absorption peak, the average total off time is shorter for 488 nm excitation (980 s) than for 532 nm excitation (1140 s) by 160 s, 75% of a standard deviation of the distribution. For the larger NCs (NC600), the averages obtained using 488 nm

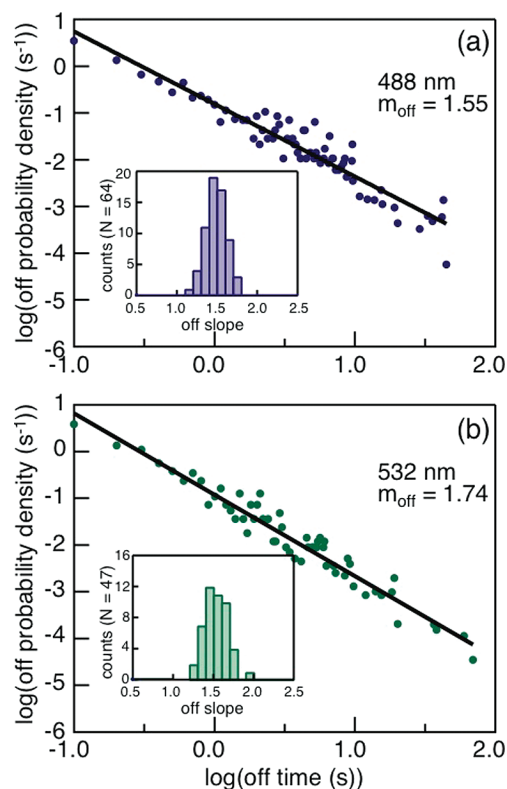


Figure 2. (a) Off-time probability density, $P(t_{\text{off}})$, shown on a log–log scale, determined from intensity trajectory shown in Figure 1c for a single NC 549 excited at 488 nm. The fit shown corresponds to a power law with exponent $m_{\text{off}} = 1.55$. Inset: Histogram of off-time slopes for all 64 individual NC549 excited at 488 nm. Table 2 reports the average and standard deviation of the slopes. (b) Off-time probability density, $P(t_{\text{off}})$, from intensity trajectory shown in Figure 1e for a single NC 549 excited at 532 nm. The fit shown corresponds to a power law with exponent $m_{\text{off}} = 1.74$. Inset: Histogram of off-time slopes for all 47 individual NC549 excited at 532 nm. Table 2 reports the average and standard deviation of the slopes.

excitation (1120 s) and 532 nm excitation (1180 s) differ by only 60 s, 25% of a standard deviation. There is similarly no difference between the distributions of total off time obtained with 532 and 405 nm excitation measured at the lower excitation rate, although the average total off time is less and the distributions are very broad with the lower excitation rate.

On-Time Distributions: Truncated Power Law Fits. We now consider the on-time distributions. Parts a and b of Figure 4 show representative on-time distributions for the larger NCs (NC600) obtained with 488 and 532 nm excitation. Instead of a pure power law, these distributions drop below the power law for long times. Consistent with diffusion-based theories,^{7,9} the distributions of on times obtained from individual NCs follow a truncated power law $P(t_{\text{on}}) = At_{\text{on}}^{-m_{\text{on}}}e^{-t_{\text{on}}/\tau_{\text{on}}}$; for the data shown, the truncation times τ_{on} are 7 and 6 s and the exponents m_{on} are 1.4 and 1.1, respectively. As with the off-time fits, τ_{on} and m_{on} were determined by fitting the logarithm of the truncated power law distribution function to the logarithm of the data. Fitting is performed by a two-step process; first the normalization A and the exponent m_{on} are determined by fitting a power law to the first six points (corresponding to time bins 0.1 to 0.6 s), and then those parameters are held fixed and τ_{on} determined. This process ensures that the shortest time points, which correspond to the largest number of events, are used to determine the power-law part of the fitting function.^{20,21}

Histograms of the τ_{on} values obtained for the individual NCs are also shown as insets to Figure 4a,b. (About 20% of the

TABLE 2: On- and Off-Time Distribution Fitting Parameters

sample	excitation		N^b	individual m_{off}		individual m_{on}			aggregated ^c	
	λ (nm)	rate (MHz)		avg	sd	N_{on}^b	avg	sd	m_{on}	τ_{on} (s)
NC549	488	0.13	64	1.5	0.1	52	1.3	0.2	1.32	20 ± 4
NC549	532	0.14	47	1.5	0.1	44	1.4	0.2	1.41	1620 ± 43
NC600	488	0.73	57	1.6	0.1	49	1.4	0.1	1.42	920 ± 42
NC600	532	0.60	85	1.5	0.1	68	1.4	0.2	1.44	920 ± 42
NC600 ^a	405	0.13	77	1.6	0.2	70	1.1	0.1	1.13	1120 ± 42
NC600 ^a	532	0.13	77	1.6	0.2	62	1.1	0.1	1.20	2120 ± 44

^aData taken at 4-fold lower absorption rate to avoid bleaching, and on glass substrate; other data sets taken on mica substrate. ^b N is the total number of NCs observed for this size and excitation, all of which gave fittable off-time distributions. N_{on} is the number which gave fittable on-time distributions, typically about 80% of the sample, as discussed in the text. ^cAverages and standard deviations are from the distribution of values obtained from fitting each individual NC. Aggregated distributions are shown in Figures 4c, 4f, and 5c and were obtained by combining together all on-events from all NCs of a given size and excitation, including the ones that did not give fittable individual on-time distributions; if the aggregated distribution omits events from those NCs which did not give fittable individual distributions, the same fit to that aggregated distribution is obtained as if all events are included. Uncertainties provided for aggregated values for τ_{on} are 20% (based on our previous⁵ examination of repeatability with multiple measurements on the same sample).

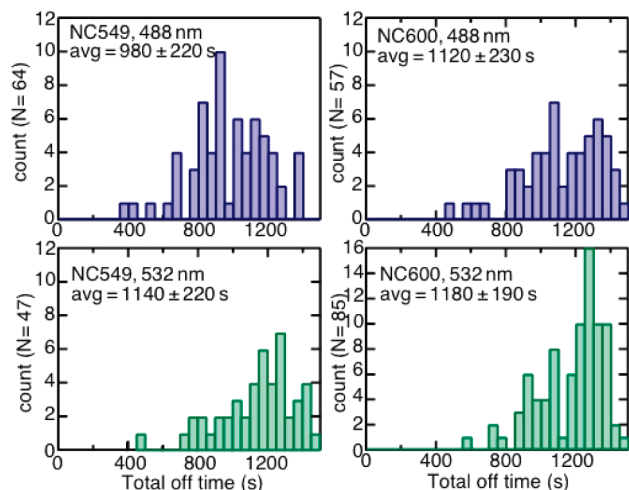


Figure 3. Distributions of total off time observed from individual NCs with 532 nm (green bars) or 488 nm (blue bars) excitation. All intensity vs time data were collected for 1500 s, and total off time was calculated from the thresholded measurements. Left column: NC549. Right column: NC600. For NC600, both 532 and 488 nm excitation are expected to lie at or above the $1P_e1P_{3/2}$ state; for NC549, 532 nm excitation falls at the absorption edge, and 488 nm excitation lies 70 meV below the expected energy of the $1P_e1P_{3/2}$ state, based on Norris and Bawendi.²²

individual on-time distributions had too few points or showed too much scatter to obtain a reliable fit; for this reason the number of truncation times is smaller than the corresponding number of off exponents reported in Figure 2. We confirmed that omitting these single-particle data from the off-time analysis has no effect on the distribution of off-time exponents. The histogram shows τ_{on} values up to 50 s; as indicated in the legend, an additional 15–20% of the NCs gave distributions with $\tau_{on} > 50$ s (12 out of 49 for 488 nm excitation, 10 out of 68 for 532 nm excitation), corresponding to essentially pure power law behavior, as the single longest recorded on time from all of the NC600 excited with 532 nm at this excitation rate is 55 s and only 8 out of 45000 events exceed 30 s. The distributions are broad, but the shapes are similar and the peaks of the distributions are comparable for the two excitation energies, roughly 6–8 s for 488 nm excitation and 4–6 s for 532 nm excitation. The exponents m_{on} for the on-time distributions fall into a much narrower range, comparable to that observed for the off-time exponents, and also show no difference for 532 or 488 nm excitation. The averages and standard deviations of m_{on} are given in Table 2.

As determining τ_{on} for the on-time distributions depends on relatively rare long-time events, we also aggregated together all of the on-time events from all single-particle data for a particular excitation energy to obtain aggregated on-time distributions, shown in Figure 4c. Fits to these aggregated distributions also show no difference between 488 and 532 nm excitation for the larger NCs. The value of τ_{on} for the aggregated distributions, 9 s, is somewhat longer than the peak value obtained from the histogram of individual truncation times, reflecting the individual on-time distributions with very long τ_{on} .

As previously described, we also measured distributions from NC600 with both 532 and 405 nm excitation at 4-fold lower absorption rate to avoid bleaching of the NCs with the 405 nm excitation. Examples of individual probability distributions, histograms of the on-time truncation times, and aggregated distributions are shown in Figure 4d–f. The on-time distributions obtained from NC600 with 532 nm at this lower absorption rate have significantly longer truncation times. As shown in Figure 4e, the peak of the distribution of individual truncation times is around 10–12 s, the distribution is broader than with higher power, and the fit to the aggregated data gives $\tau_{c,on} = 21$ s. Compared to excitation with 532 nm at higher power, a similar fraction of the individual probability distributions (10 out of 62, or 16%) have $\tau_{on} > 50$ s, but more have τ_{on} between 25 and 50 s.

With 405 nm excitation (Figure 4d), the distribution of individual truncation times is narrower and peaked at shorter times (around 4–6 s), although a similar number of individual NCs (12 out of 70, or 17%) have $\tau_{on} > 50$ s. In addition, τ_{on} for the aggregated distribution is 11 s (Figure 4f), much shorter than for 532 nm excitation at this reduced excitation rate. By all measures, the distribution of on-events cuts off at shorter times with this higher-energy excitation. We thus find that exciting the larger size NCs at either 532 or 488 nm, corresponding to 270 and 480 meV above the band gap respectively, gives equivalent on-time distributions, while exciting at 405 nm, about 1 eV above the band gap, shortens the distribution of on-time truncation times.

The smaller size NCs (NC549) also show truncated power law on-time distributions, with a very wide range of truncation times, and many longer truncation times than those observed with the larger NCs at a comparable excitation rate. Figure 5 shows the on-time probability distributions obtained at 488 and 532 nm corresponding to the intensity-time traces from NC549 shown in Figure 1. (We were unable to obtain data from NC549

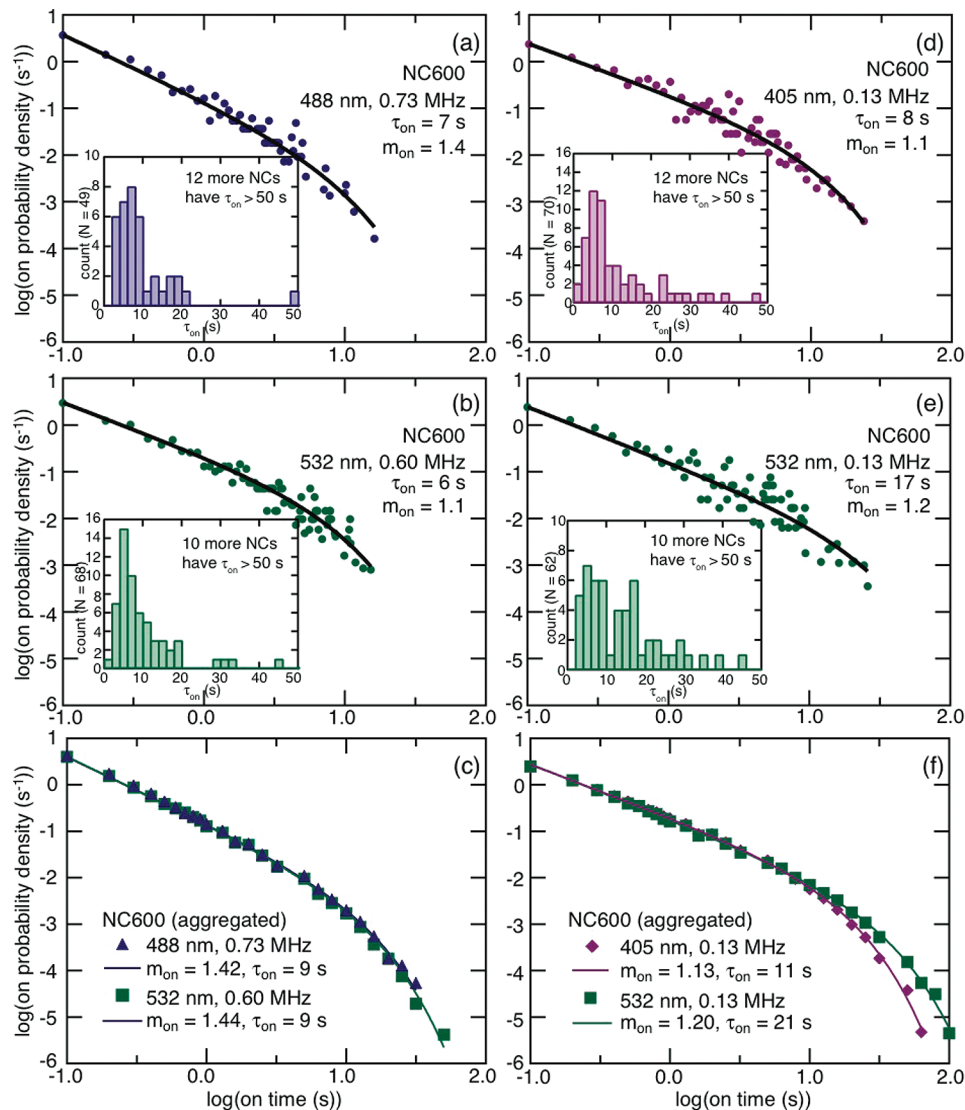


Figure 4. (a) On-time probability density, $P(t_{\text{on}})$, shown on a log–log scale, for a single NC 600 excited at 488 nm and 0.73 MHz excitation rate. The fit shown corresponds to a truncated power law with $m_{\text{on}} = 1.4$ and $\tau_{\text{on}} = 7$ s. Inset: Histogram of τ_{on} values for 49 individual NC600 excited at 488 nm; 12 out of the 49 (26%) have $\tau_{\text{on}} > 50$ s. Table 2 reports the average and standard deviation of the exponents m_{on} . (b) On-time probability density, $P(t_{\text{on}})$, for a single NC 600 excited at 532 nm and 0.60 MHz excitation rate. The fit shown corresponds to a truncated power law with $m_{\text{on}} = 1.1$ and $\tau_{\text{on}} = 6$ s. Inset: Histogram of τ_{on} values for 68 individual NC600 excited at 488 nm; 10 out of the 68 (15%) have $\tau_{\text{on}} > 50$ s. Table 2 reports the average and standard deviation of the exponents m_{on} . (c) Aggregated on-time probability density, $P_{\text{agg}}(t_{\text{on}})$, obtained by combining all on events for all NC600 excited at 488 nm (blue symbols) and for all excited at 532 nm (green symbols) with 0.60 MHz excitation rate. (d) On-time probability density, $P(t_{\text{on}})$, for a single NC 600 excited at 405 nm and 0.13 MHz excitation rate. The fit shown corresponds to a truncated power law with $m_{\text{on}} = 1.1$ and $\tau_{\text{on}} = 8$ s. Inset: Histogram of τ_{on} values for 68 individual NC600 excited at 488 nm; 12 out of the 70 (17%) have $\tau_{\text{on}} > 50$ s. Table 2 reports the average and standard deviation of the exponents m_{on} . (e) On-time probability density, $P(t_{\text{on}})$, for a single NC 600 excited at 532 nm and 0.13 MHz excitation rate. The fit shown corresponds to a truncated power law with $m_{\text{on}} = 1.2$ and $\tau_{\text{on}} = 17$ s. Inset: Histogram of τ_{on} values for 62 individual NC600 excited under these conditions; 10 out of the 62 (20%) have $\tau_{\text{on}} > 50$ s. Table 2 reports the average and standard deviation of the exponents m_{on} . (f) Aggregated on-time probability density, $P_{\text{agg}}(t_{\text{on}})$, obtained by combining all on events for all NC600 excited at 405 nm (violet symbols) and for all excited at 532 nm with 0.13 MHz excitation rate (green symbols).

using 405 nm excitation because of rapid bleaching of these smaller NCs.) Histograms of the individual truncation times τ_{on} for values up to 50 s are shown in the insets to Figure 5a,b; an additional 20 values out of 52 (38%) for 488 nm and 10 values out of 44 (23%) for 532 nm exceed 50 s.

Although the distributions are too broad to allow a precise comparison, the distributions obtained with 488 and 532 nm are very similar. There are minor differences: the τ_{on} histogram obtained using 532 nm excitation is slightly shifted to lower values, and a somewhat smaller fraction of the values exceed the range shown in the histogram. For the aggregated data for the NC549, shown in Figure 5c, the truncation time obtained with 532 nm is likewise somewhat shorter, 16 s, compared to

20 s obtained with 488 nm. However, the difference in τ_{on} for the aggregated data is within the 20% uncertainty based on our previous study⁵ of the reproducibility of τ_{on} values for aggregated data, and the distributions are similar. The greater total off time observed with 532 nm excitation of NC549 may also reduce the observed τ_{on} simply by reducing opportunities for long on times within the same overall measurement time. Consequently, the primary conclusion to be drawn from these data is that exciting at or near the band gap gives rise to a broad distribution of truncation times, and for this size of NC, exciting at 210 meV above the band gap increases the total on time slightly but does not make a significant difference in the statistics.

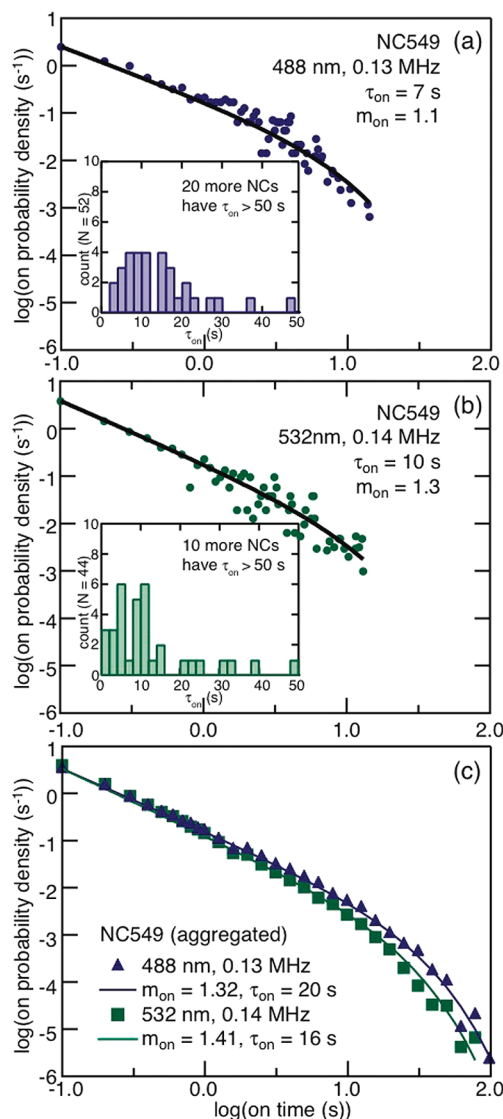


Figure 5. (a) On-time probability density, $P(t_{\text{on}})$, for a single NC 549 excited at 488 nm (intensity trajectory shown in Figure 1c). The fit shown corresponds to a truncated power law with exponent $m_{\text{on}} = 1.1$ and $\tau_{\text{on}} = 7$ s. Inset: Histogram of on-time truncation times for 52 individual NC600 excited at 488 nm; 20 out of the 52 (38%) have $\tau_{\text{c}} > 50$ s. Table 2 reports the average and standard deviation of the exponents m_{on} . (b) On-time probability density, $P(t_{\text{on}})$, for a single NC549 excited at 532 nm (intensity trajectory shown in Figure 1e). The fit shown corresponds to a truncated power law with exponent $m_{\text{on}} = 1.3$ and $\tau_{\text{on}} = 10$ s. Inset: Histogram of on-time truncation times for 44 individual NC600 excited at 532 nm; 10 out of the 44 (23%) have $\tau_{\text{on}} > 50$ s. Table 2 reports the average and standard deviation of the exponents m_{on} . (c) Aggregated on-time probability density, $P_{\text{agg}}(t_{\text{on}})$, obtained by combining all on events for all NC532 excited at 488 nm (blue symbols) and for all excited at 532 nm (green symbols). Table 2 reports uncertainties.

Discussion

Off Times: Insensitivity to Excitation Energy. For the larger size of nanocrystal (NC600), we find no difference in off-time power-law exponents or total off times (for a given excitation power level) at any wavelength. Measurements of size dependence of the electronic structure of CdSe NCs by Norris and Bawendi²² suggest that for NCs with peak emission at 600 nm, 532 nm excitation should roughly correspond to the $1P_{3/2}1P_e$ state, so all three excitations correspond to exciting the NC at the $1P_{3/2}1P_e$ state or higher. The off-time results therefore suggest that the mechanism by which a dark NC returns to the bright

state is insensitive to excitation energy when the excitation is at or above the $1P_{3/2}1P_e$ state.

For the smaller nanocrystals (NC549), although we find no difference in the off-time exponents, we do find somewhat greater total off times when exciting at the absorption edge (532 nm), compared to exciting near, though somewhat (70 meV) below, the expected $1P_{3/2}1P_e$ state (488 nm). Whether the excitation energy falls above or below the $1P_{3/2}1P_e$ state is expected to affect the off times in a diffusion-controlled model involving Auger-assisted detrapping.²³ In this model, the dark state corresponds to a trapped hole state, and detrapping is enhanced when the transition from the trap to the valence band is resonant with the $1P_e$ to $1S_e$ relaxation transition for a core electron. If the $1P_{3/2}1P_e$ state is energetically inaccessible, the lifetime of the dark state is prolonged.²³ Attributing nonradiative recombination to surface hole trapping when the $1P_{3/2}1P_e$ state is excited is consistent with ultrafast measurements of carrier dynamics by the Klimov²⁴ and Kambhampati²⁵ groups.

The excitation energy dependence of the total off time shown in Figure 3 is consistent with this model, as the total off time distribution for NC549 shifts to longer times with 532 nm excitation, while it is unaffected for the larger NC600 for which all excitations are expected to be above the $1P_{3/2}1P_e$ state. However, the effect is small enough that it may simply be due to statistical variation. As 488 nm is still expected to be 3kT below the $1P_{3/2}1P_e$ state, based on the Norris and Bawendi measurements²² (532 nm is expected to be 11kT below the $1P_{3/2}1P_e$ state), it is not surprising that any effect would be small. Further experiments, including measurement of individual NC spectra and direct determination of the $1P_{3/2}1P_e$ energy level for the samples studied, are necessary to explore this matter further.

On Times: Evidence for Different Energy Regimes of Fluorescence Dynamics. For the larger size of nanocrystal (NC600), we find that the on-time distributions are very similar for 532 and 488 nm, excitation roughly at the $1P_e1P_{3/2}$ state and somewhat (210 meV) above, while the truncation times shorten appreciably with a much higher energy excitation (405 nm, nearly 700 meV above the $1P_{3/2}1P_e$ state). These findings indicate that excess energy of the exciting photon does not necessarily affect the blinking statistics; instead, the position of the excitation energy within the energy level structure of the NC is important.

Previous measurements of the energy dependence of spectral diffusion of single NC spectra are consistent with this finding. Spectral diffusion has been shown to be correlated with blinking²⁶ and plays a key role in several proposed blinking mechanisms.^{7,9} In addition, spectral diffusion is attributed to fluctuations in the local electric field due to charge rearrangement at the surface of the NC,^{26–28} another model of blinking, the fluctuating barrier mechanism, involves local electric field fluctuations.³ Empedocles and Bawendi²⁷ investigated the excitation energy and intensity dependence of single NC linewidths due to spectral diffusion, at both low temperature and room temperature. They found that at low temperature, increasing excitation energy by 250 meV, or increasing excitation intensity, caused a corresponding increase in the line width, but at room temperature, they found that the line width was independent of excitation intensity (they did not report energy-dependence measurements). They concluded that at room temperature, spectral diffusion was driven by thermal surface charge rearrangement, while at low temperature, phonons excited by the excess energy of the exciton were involved in surface charge rearrangement. Consequently, their measurements sug-

gest that the rate of spectral diffusion at room temperature should not be affected by the excess energy of the exciting phonon.

Our measurements on the smaller nanocrystals (NC549) correspond to exciting at the absorption edge (532 nm) and ~ 70 meV below the $1P_{3/2}1P_e$ state (488 nm). We observe (Figure 5) that the distribution of truncation times is shifted slightly to shorter times with 532 nm excitation than with 488 nm excitation. However, this difference lies within the 20% uncertainty we estimate for aggregated measurements of truncation times, based on the reproducibility of separate measurements and repeated sampling within a larger distribution.⁵ Furthermore, it is possible that the difference arises solely because the total amount of time spent off is somewhat greater with 532 nm excitation, and thus the on-time distributions appear to cut off slightly earlier simply due to sampling fewer on times. The difference between the (very broad) distributions of individual τ_{on} values is small, as is the difference between the aggregated on-time distributions. Consequently, we interpret these results as indicating that there is little or no difference in the on-time distributions, except what may be imposed by the increased amount of time off, for two excitation energies below the $1P_{3/2}1P_e$ state.

The absorption rate for NC549 is comparable to that used with the lower power measurements on NC600. Here we see that although the truncation times obtained for both sizes with 532 nm excitation are comparable, the average on-time power-law exponent with the larger NC600 is 1.1 while it is 1.3 for the NC549, reflecting substantially more total time on. In addition, the distributions of individual τ_{on} values are very broad for excitation near the band gap while they are narrower for excitation well above the band gap.

While this study was underway, Knappenberger et al. reported measurements on the wavelength dependence of on-time distributions, obtained with a tunable laser.⁶ They measured on-time distributions from nanocrystals of similar size to our NC600 (absorption peak at 580 nm, emission peak at 610 nm) at four different wavelengths and found that the on-time distributions followed a pure power law for excitation energies 124 or 162 meV above the band gap but showed clear truncation with truncation times of roughly 4 or 6 s for energies 250 or 330 meV above the band gap. They attributed this to a threshold of excitation energy, above which the excited electron can access a different set of trap states that limit the maximum on-time.

Our work is consistent with the suggestion of Knappenberger et al. that there are distinct regimes of excitation energy in which blinking statistics differ, if the boundary between the two excitation energy regimes corresponds to the $1P_{3/2}1P_e$ state. In addition, our work indicates that exciting very far above the band gap may enter a third.

To identify a mechanism for how the position of the excitation energy within the NC energy level structure might affect blinking dynamics, we consider previous measurements of the excitation energy dependence of NC quantum yield. In ensemble photoluminescence excitation (PLE) measurements, Hoheisel and co-workers¹⁷ observed a reduction in luminescence efficiency for NCs excited above a state they identify as the second excited state. They interpreted their results as indicating that an additional, quasicontinuous band of states with different fluorescence dynamics becomes available at energies corresponding to the $1P_{3/2}1P_e$ state. At still higher energies, the PLE spectrum becomes independent of the exciting photon energy. Comparable results were recently obtained by Cooney et al.,¹⁸ and similar trends have subsequently been observed by Ellingson et al. in InP nanocrystals²⁹ and by Dias et al. in CdSe/ZnS/

CdSe core/barrier/shell nanocrystals,³⁰ although there is some disagreement in the literature, as Tonti et al.³¹ do not observe this dependence. Recent time-resolved studies by Sewall et al.²⁵ also indicate that surface hole trapping rates in CdSe NCs increase significantly with excess electronic energy at and above the $1P_{3/2}1P_e$ state.

Our finding that the NC600 truncation time shortens with 405 nm excitation suggests that there could be a second, higher energetic threshold present, above which additional trap states or dynamic pathways become available. The 405 nm excitation is about 1 eV above the band gap, which is well into the energy-independent region of the bulk photoluminescence spectrum reported by Hoheisel et al.¹⁷ but not high enough to reach the states in the ZnS shell. This energy-independent region of the PLE spectrum could correspond to a truly continuous, high-energy range of exciton energy states, and when the exciton reached these states this could produce a shorter cutoff to the on-time distribution. Alternatively, the near-ultraviolet excitation could more readily modify or detach the surface ligands or otherwise create new surface traps, modifying the fluorescence dynamics.³²

Our results with NC600 at higher power are broadly consistent with the results of Knappenberger et al. The peaks of the truncation time distributions we observe with 532 and 488 excitation are comparable, although we also observe some NC600 which show very long truncation times even when excited at 488 or 405 nm. The wider variation we observe in the individual NC truncation times may be due to the different substrate we use (Knappenberger et al. used a silanized glass substrate, while we used fresh mica or cleaned glass substrates, neither of which was chemically passivated). We have previously observed differences in truncation times between nanorods on mica and silicon nitride substrates, though not between mica and bare glass.²⁰ This suggests that the truncation time is determined in part by the environment of the NC.

For excitation near the band gap, Knappenberger et al. report pure power law on-time distributions, rather than truncated power law distributions.⁶ We find that with NC549, the typical truncation times are very long (60% have $\tau_{on} > 16$ s), but most of our individual NC on-time distributions can still be described by a truncated power law, and again the distributions are broad. As our measurements are 1500 s long, rather than 600 s in the Knappenberger et al. study of NCs, the finite τ_{on} we observe may be attributable to the combination of our greater measurement time along with the wider variation we observe from NC to NC.

Another difference between our findings and those of Knappenberger et al. is that we observe that the on-time probability distributions depend somewhat on the excitation intensity and hence the excitation rate, as shown in the changes in both truncation time and power-law exponent observed for the 532 and 405 nm measurements on NC600 at 4-fold lower excitation rate. Our findings of the intensity dependence are consistent with those recently reported by Peterson and Nesbitt.¹¹ As our NC600 measurements were made at intensities comparable to the lowest used by Knappenberger et al., the difference may reflect differing regimes of intensity dependence, as proposed by Peterson and Nesbitt.¹¹ Further work will be required to distinguish the effects of excitation energy and excitation rate. It is also possible that the difference in substrate preparation may contribute.

To identify more conclusively the role of excitation energy in the on-time blinking dynamics, future studies will examine an intermediate size of nanocrystal, for which 532 nm excitation

should lie below the $1P_{3/2}1P_e$ state and 488 nm excitation should lie above the $1P_{3/2}1P_e$ state. Future studies will also involve spectral measurements to determine whether there is any correlation between the spectrum of the individual nanoparticle or the amount of spectral diffusion and the truncation time.

Conclusions

In conclusion, we find that for two different sizes of nanocrystals, excitation energy does not affect the power-law form or exponents of the blinking off-time probability distributions, but exciting at the band gap increases the average total time off by 160 s (75% of a standard deviation), compared to exciting 210 meV above the band gap.

For the on-time distributions, with comparable excitation rates, the on-time truncation times τ_{on} are very similar for the larger nanocrystals excited either 270 or 480 meV above the band gap and likewise are very similar for the smaller nanocrystals excited either at the band gap or 210 meV above the band gap. However, exciting the larger nanocrystals approximately 1 eV above the band gap gives shorter τ_{on} than exciting 270 meV above the band gap.

These findings indicate that simply increasing the excitation energy for a given excitation rate does not change the blinking dynamics, consistent with measurements of energy and intensity dependence of spectral diffusion, in which the amount of excess energy does not affect the rate of spectral diffusion at room temperature. Our findings are consistent with differing regimes of blinking dynamics for excitation energies below and above the $1P_eP_{3/2}$ level and possibly a third such regime at much higher energy. These regimes correspond to previously observed changes in luminescence efficiency, most likely corresponding to energies at which the exciton can access additional trap states or other dynamical pathways. These results also support spectral diffusion-based models for nanocrystal blinking, because the sensitivity of the blinking on-time statistics to excitation energy appears to depend on the position of the excitation within the NC energy spectrum.

Acknowledgment. This work was supported by startup funds provided by Swarthmore College, the HHMI grant to Swarthmore College for undergraduate summer research support, and partial support by the NSF CAREER Award DMR-0449533 and ONR YIP N000140410489. We thank Rudolph Marcus, Pavel Frantsuzov, and Michel Orrit for theoretical advice; Carl Grossman for experimental assistance and feedback on the manuscript; Jeffrey Peterson, Patanjali Kambhampati, Claudia Querner, and Peter Collings for helpful discussions; Ken Kuno and Vladimir Protasenko for valuable experimental advice; Orion Sauter for assistance with data analysis; and Douglas Jahn and Coherent Inc. for the loan of the Sapphire laser.

References and Notes

- (1) Cichos, F.; von Borczyskowski, C.; Orrit, M. *Curr. Opin. Colloid Interface Sci.* **2007**, *12*, 272, and references therein.
- (2) Frantsuzov, P.; Kuno, M.; Janko, B.; Marcus, R. A. *Nat. Phys.* **2008**, *4*, 519–522, and references therein.
- (3) Kuno, M.; Fromm, D. P.; Hamann, H. F.; Gallagher, A.; Nesbitt, D. J. *J. Chem. Phys.* **2000**, *112*, 3117. Kuno, M.; Fromm, D. P.; Hamann, H. F.; Gallagher, A.; Nesbitt, D. J. *J. Chem. Phys.* **2001**, *115*, 1028. Kuno, M.; Fromm, D. P.; Johnson, S. T.; Gallagher, A.; Nesbitt, D. J. *Phys. Rev. B* **2003**, *67*, 125304.

- (4) Shimizu, K. T.; Neuhauser, R. G.; Leatherdale, C. A.; Empedocles, S. A.; Woo, W. K.; Bawendi, M. G. *Phys. Rev. B* **2001**, *63*, 205316.
- (5) Wang, S.; Querner, C.; Emmons, T.; Drndic, M.; Crouch, C. H. *J. Phys. Chem. B* **2006**, *110*, 23221–23227.
- (6) Knappenberger, K.; Wong, D.; Romanyuk, Y.; Leone, S. *Nano Lett.* **2007**, *7*, 3869. Knappenberger, K.; Wong, D.; Xu, W.; Schwartzberg, A.; Wolcott, A.; Zhang, J.; Leone, S. *ACS Nano* **2008**, *2*, 2143.
- (7) Tang, J.; Marcus, R. A. *Phys. Rev. Lett.* **2005**, *95*, 107401. Tang, J.; Marcus, R. A. *J. Chem. Phys.* **2005**, *123*, 054704. Tang, J.; Marcus, R. A. *J. Chem. Phys.* **2005**, *123*, 204511.
- (8) In the diffusion-controlled electron transfer theory of Tang and Marcus, there are two characteristic times, the truncation or saturation time and the critical time. The truncation time is notated as $1/\Gamma$ in their work, to distinguish it from the critical time, notated t_c ; the critical time is much shorter. (Recent experiments suggest that the critical time is on the order of a few milliseconds.) We will notate the truncation time as τ_{on} .
- (9) Frantsuzov, P. A.; Marcus, R. A. *Phys. Rev. B* **2005**, *72*, 155321.
- (10) Stefani, F. D.; Zhong, X.; Knoll, W.; Kreiter, M.; Han, M. *Phys. Rev. B* **2005**, *72*, 125304.
- (11) Peterson, J. J.; Nesbitt, D. J. *Nano Lett.*, in press.
- (12) Efros, A.; Rosen, M. *Phys. Rev. Lett.* **1997**, *78*, 1110.
- (13) Hammer, N. I.; Early, K. T.; Sill, K.; Odoi, M. Y.; Emrick, T.; Barnes, M. D. *J. Phys. Chem. B* **2006**, *110*, 14167.
- (14) Park, S. J.; Link, S.; Miller, W. L.; Gesquiere, A.; Barbara, P. F. *Chem. Phys.* **2007**, *341*, 169.
- (15) Verberk, R.; van Oijen, A. M.; Orrit, M. *Phys. Rev. B* **2002**, *66*, 233202.
- (16) Two lots of these NCs were used; the first lot was used for the measurements shown in Figure 4a–c and had an absorption peak at 583 nm and an emission peak at 602 nm. The second lot was used for the measurements in Figure 4d–f and had an absorption peak at 584 nm and an emission peak at 595 nm. The absorption spectrum from the first lot is shown in Figure 1.
- (17) Hoheisel, W.; Colvin, V. L.; Johnson, C. B.; Alivisatos, A. P. *J. Chem. Phys.* **1994**, *101*, 8455.
- (18) Cooney, R. R.; Sewall, S. L.; Sagar, D.; Kambhampati, P. *Phys. Rev. Lett.* **2009**, *102*, 127404.
- (19) Yu, W. W.; Qu, L.; Guo, W.; Peng, X. *Chem. Mater.* **2003**, *15*, 2854.
- (20) Wang, S.; Querner, C.; Willis, L.; Fischbein, M.; Novikov, D.; Crouch, C. H.; Drndic, M. *Nano Lett.* **2008**, *8*, 4020.
- (21) Tang, J. *J. Phys. Chem. A* **2007**, *111*, 9336.
- (22) Norris, D. J.; Bawendi, M. G. *Phys. Rev. B* **1996**, *53*, 16338.
- (23) Marcus, R. A. On the Theory of Intermittent Fluorescence of Quantum Dots. Plenary lecture at 5th International Symposium on the Theory of Atomic and Molecular Clusters, Richmond, VA, May 2007.
- (24) Klimov, V. I.; Schwarz, C. J.; McBranch, D. W.; Leatherdale, C. A.; Bawendi, M. G. *Phys. Rev. B* **1999**, *60*, R2177. Klimov, V. I. Charge Carrier Dynamics in Nanocrystal Quantum Dots. In *Semiconductor and Metal Nanocrystals: Synthesis and Electronic and Optical Properties*; Klimov, V. I., Ed.; Marcel Dekker: New York, 2004; Ch. 5.
- (25) Sewall, S. L.; Cooney, R. R.; Anderson, K.; Dias, E.; Sagar, D. M.; Kambhampati, P. *J. Chem. Phys.* **2008**, *129*, 084701.
- (26) Neuhauser, R. G.; Shimizu, K. T.; Woo, W. K.; Empedocles, S. A.; Bawendi, M. G. *Phys. Rev. Lett.* **2000**, *85*, 3301.
- (27) Empedocles, S. A.; Bawendi, M. G. *J. Phys. Chem. B* **1999**, *103*, 1826.
- (28) Gomez, D.; van Embden, J.; Mulvaney, P. *Appl. Phys. Lett.* **2006**, *88*, 154106.
- (29) Ellingson, R.; Blackburn, J. L.; Yu, P.; Rubles, G.; Micic, O.; Nozik, A. J. *J. Phys. Chem. B* **2002**, *106*, 7758.
- (30) Dias, E. A.; Sewall, S. L.; Kambhampati, P. *J. Phys. Chem. C* **2007**, *111*, 708. Cooney, R. R.; Sewall, S. L.; Dias, E. A.; Sagar, D.; Anderson, K. E. H.; Kambhampati, P. *Phys. Rev. B* **2007**, *75*, 245311.
- (31) Tonti, D.; van Mourik, F.; Chergui, M. *Nano Lett.* **2004**, *4*, 2483.
- (32) The highest energy excitation used by Knappenberger et al.⁶ in their initial study corresponded to 525 nm, so they did not explore this higher energy regime with spherical NCs. In a follow-up study of excitation energy dependence in tetradecylphosphonic acid-capped CdSe nanorods, they saw no difference between 400 nm excitation and 510 nm excitation. However, the truncation times observed with NRs are so much shorter (of order 1 s) that it is possible that whenever the new dynamics are introduced by the high-energy excitation, they only operate on the longer (~ 10 s) timescale we observe.